PNNL-34858

Operator-theoretic Resilience Calculations (ORC)

Technical Report

December 22, 2023

Sai Pushpak Nandanoori
Subhrajit Sinha
Craig Bakker
Thiagarajan Ramachandran
Bowen Huang

U.S. DEPARTMENT OF ENERGY

Prepared for the U.S. Department of Energy
Under contract DE-AC05-76RL01830

PACIFIC NORTHWEST NATIONAL LABORATORY
operated by
BATTELLE
for the
UNITED STATES DEPARTMENT OF ENERGY
under Contract DE-AC05-76RL01830

Printed in the United States of America

Available to DOE and DOE contractors from
the Office of Scientific and Technical Information,
P.O. Box 62, Oak Ridge, TN 37831-0062
www.osti.gov
ph: (865) 576-8401
fox: (865) 576-5728
email: reports@osti.gov

Available to the public from the National Technical Information Service
5301 Shawnee Rd., Alexandria, VA 22312
ph: (800) 553-NTIS (6847)
or (703) 605-6000
email: info@ntis.gov
Online ordering: http://www.ntis.gov

PNNL-34858

Operator-theoretic Resilience Calculations (ORC)

Technical Report

December 22, 2023

Sai Pushpak Nandanoori
Subhrajit Sinha
Craig Bakker
Thiagarajan Ramachandran
Bowen Huang

Prepared for
the U.S. Department of Energy
Under Contract DE-AC05-76RL01830

Pacific Northwest National Laboratory
Richland, Washington 99352

Acronyms and Abbreviations

ORC	Operator-theoretic Resilience Calculations
PNNL	Pacific Northwest National Laboratory
PFO	Perron-Frobenius Operator
KO	Koopman Operator

Acknowledgments

This research was supported by the **Resilience through Data-driven intelligently-Designed Control (RD2C) Initiative**, under the Laboratory Directed Research and Development (LDRD) Program at Pacific Northwest National Laboratory (PNNL). PNNL is a multi-program national laboratory operated for the U.S. Department of Energy (DOE) by Battelle Memorial Institute under Contract No. DE-AC05-76RL01830. The authors thank Aditya Ashok (while he was with PNNL), Rohit Jinisiwale, Thomas Edgar and their team from the RD2C initiative for helping us obtain the data from the HYPERSIM simulation.

Contents

Figures

1.0 Introduction

Resilience is similar to robustness and reliability, but it deals with large disruptions rather than small ones [1]. There are also multiple aspects to resilience [1], which means that it is hard to capture with a single definition. The various definitions and measures of resilience should therefore be thought of as components of resilience or even necessary conditions for resilience rather than complete encapsulations of resilience or sufficient conditions for resilience [2]. Resilience is defined as the ability to maintain critical system functions in the midst of large disruptions [3–5] and as the ability to quickly and fully recover from such disruptions [6–8]. Occasionally, preparation before or anticipation of a disruption can also be considered a form of resilience [1].

Resilience is hard to quantify: there are many different descriptions of resilience, and even once a definition has been chosen, it may not be straightforward to write out that definition in a mathematical form. The resilience metrics in the literature can be either generic or model-specific. Model-specific metrics are limited to the scope of their respective models, but even generic metrics require user input in the form of performance measures (operating cost, efficiency, etc.) and/or an explicit prioritization of system functions (depending on the resilience definition being used) in order to be calculated. Some of these metrics relate to system stability (e.g., the size of a basin of attraction) [6] or to controllability [4, 9], which are both difficult to calculate for general nonlinear systems. Moreover, the metrics in the literature are generally formulated as *post hoc* assessment tools, not predictive metrics. They are not designed to inform real-time control decisions in general control systems. A recent exception to this used the Koopman Operator (KO) to apply linear controllability and observability analyzes to general nonlinear systems and thereby derive a generalizable resilience metric by considering a ratio of observability to controllability [2].

1.1 The Koopman Operator

The Koopman Operator (KO) is an infinite-dimensional mathematical construct that maps nonlinear dynamical systems to a space in which the dynamics become linear [10]. Recent works [11] show promise in studying nonlinear dynamical system in a higher-dimensional abstract space using the KO and the Perron-Frobenius Operator (PFO). The KO and PFO are adjoint to each other, but the KO is more commonly used than the PFO for data-driven discovery and analysis of dynamical systems. Recent works such as [12, 13] extend these methods to study nonlinear systems from data with noisy measurements and when there is sparse data. Data-driven KO representations can then be used for tasks such as phase space analysis [14], studying equivariance [12], and global stability analysis [15], finding observability gramians/observers [16] among others. KO theory can also be extended to controlled systems [17–20].

Operator-theoretic methods provide a structured, data-driven way to represent dynamical system behavior. This structure both provides analytical insight and enables the use of a wide range of computational methods [10]. Operator-theoretic methods have been used to assess controllability [21], observability [22], and nonlocal stability [23]. Some initial work has also been done on resilience more generally [2]. This report builds on those contributions, as well as power grid applications of operator theoretic methods [24, 25], in using operator-theoretic methods to measure system resilience.

1.2 Objectives of this Project

Develop operational metrics to characterize the resilience of a dynamic network in real-time from time-series data.

1. Resilience ratio
2. Recovery energy

Resilience analysis developed under this project considers the controllability and observability and provides a real-time understanding of resilience without creating/simulating the system model.

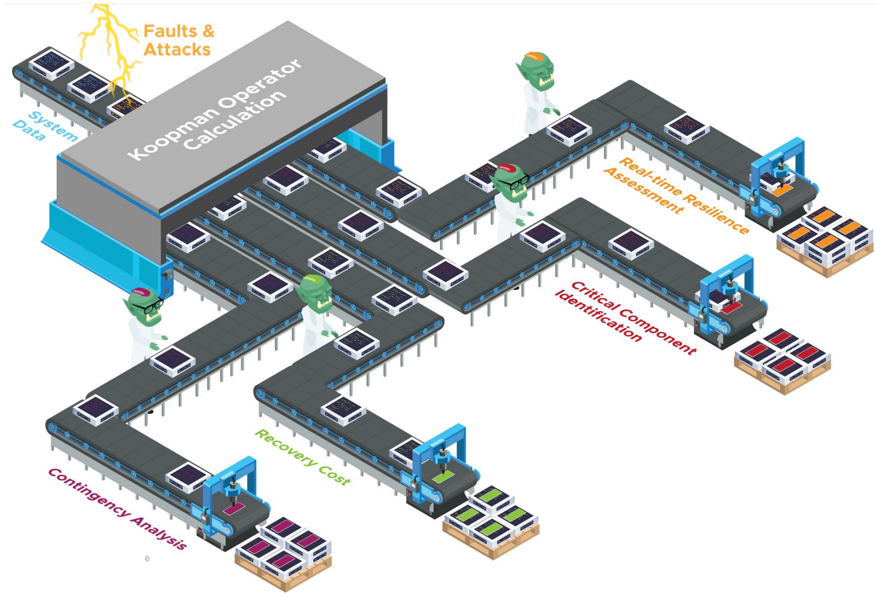

Figure 1: Capability overview of ORC.

1.3 Objectives of this Report

The objective of this report is to discuss the validation study of the resilience metrics developed under this project. The data for the validation study is obtained from the HYPERSIM simulation generated under the RD2C initiative.

For detailed technical details of the development of the resilience metrics, we refer the readers to [26] and [27].

2.0 Resilience Metrics

We begin by recalling the resilience metrics developed under this project from [26] and [27].

Background

Consider the input-output system

$$\dot{x} = f(x) + \sum_{i=1}^{p} g_i(x) u_i, \quad y = h(x), \tag{1}$$

The controlled nonlinear system (1) has its Koopman linear representation as

$$\dot{z} = Az + \tilde{B}u, \quad y = C^h z, \tag{2}$$

where $\tilde{B} = [\tilde{B}_1, \cdots, \tilde{B}_p] \in \mathbb{R}^{d \times p}$.

2.1 Resilience Ratio

The resilience ratio is defined as a ratio of the energy required to observe and the energy required to control. Given a controllable and observable nonlinear system of the form (1) and its Koopman representation (2), the resilience of a state x is defined as

$$R(x) := \frac{x^T X_o x}{x^T X_c^{-1} x}, \tag{3}$$

where X_c and X_o are the controllability and observability Gramians of the original nonlinear system, respectively.

The resilience of a control dynamical system of the form (1) is given by

$$R := \mathrm{tr}(X_r) = \mathrm{tr}(X_o^{\frac{1}{2}} X_c X_o^{\frac{1}{2}}). \tag{4}$$

Degree of resilience with respect to resilience ratio: Easy to Observe (maximum output energy) and Easy to Control (minimum input energy).

2.2 Recovery Energy

Energy to recovery is defined as the minimum input energy required to steer the system from the disturbance state to the post restoration state. The recovery energy is computed by solving the following convex optimization problem.

$$\begin{aligned} E_{N,M}(x) = \min_{u(i)} & \sum_{i=1}^{N} u(i)^T C_u u(i) \\ s.t \;\; & z(i+1) = Kz(i) + Bu(i) \\ & z(0) = \psi(x) \\ & z(i) \in \psi(S), \; N \le i \le N + M \; u(i) \\ & = 0, \; N \le i \le N + M \\ & u(i) \in U \subset \mathbb{R}^m, \; 1 \le i \le N + M. \end{aligned} \tag{5}$$

Degree of resilience with respect to recovery energy is the amount of input energy needed to recover. For more details on computing the resilience metrics discussed above, we refer the readers to [26] and [27].

2.3 Application of Resilience Metrics

The disturbance propagation phase in power systems is usually classified into pre-disturbance resilient state, disturbance propagation state and post-restoration state. Furthermore, the disturbance propagation state is further divided into disturbance progress, post-disturbance degraded state and restorative state. All these states of operation results in a resilience trapezoid as shown in Fig. 2.

The resilience ratio metric developed under this project is applied in a pre-disturbance state. Applying this metric, one can study/analyze the effect of losing a sensor (measuring device such as a PMU) or an actuator (inverter or a generator). This helps take proactive control actions to achieve a highly resilient system.

Another resilience metric, the recovery energy is computed by taking an initial condition from the post-disturbance. For instance, this metric can be applied immediately after a fault to understand the minimum amount of energy required to recover and maintain the desired operating state for a given future time window.

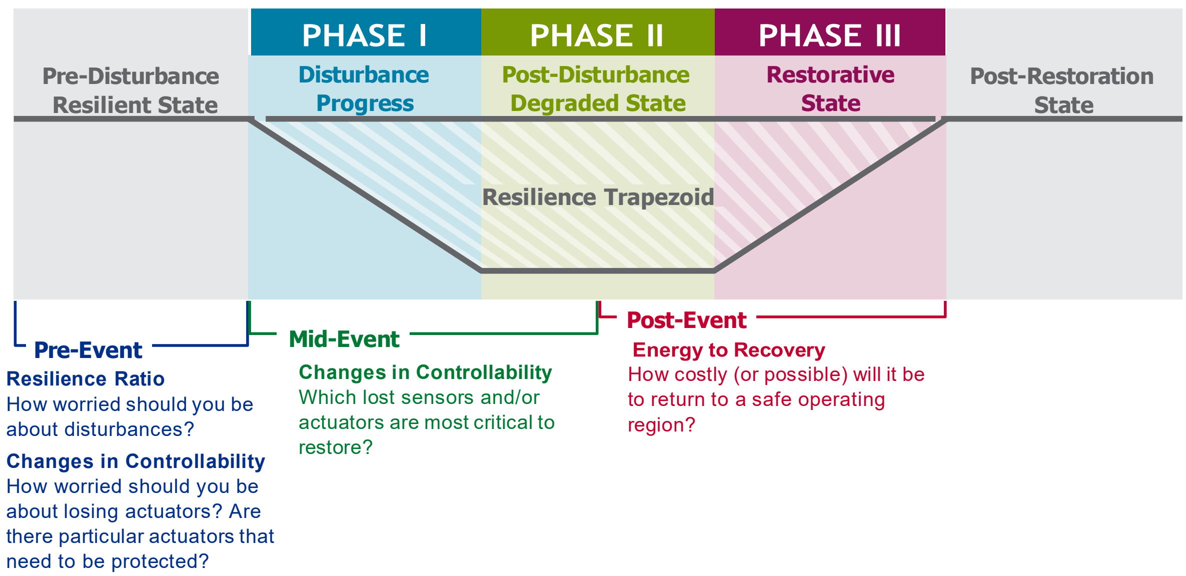

Figure 2: Higher level overview of resilience metric applications to power systems.

3.0 Resilience Metric Validation

The 123-bus networked microgrid is considered and the team modeled it with 3 diesel generators (DGs), 3 Grid-forming inverters (GFMs), and 3 Grid-following inverters (GFLs) on the HYPERSIM by OPAL-RT. The resultant network is shown in Fig. 3 and for more details on this testbed, we refer the readers to [28].

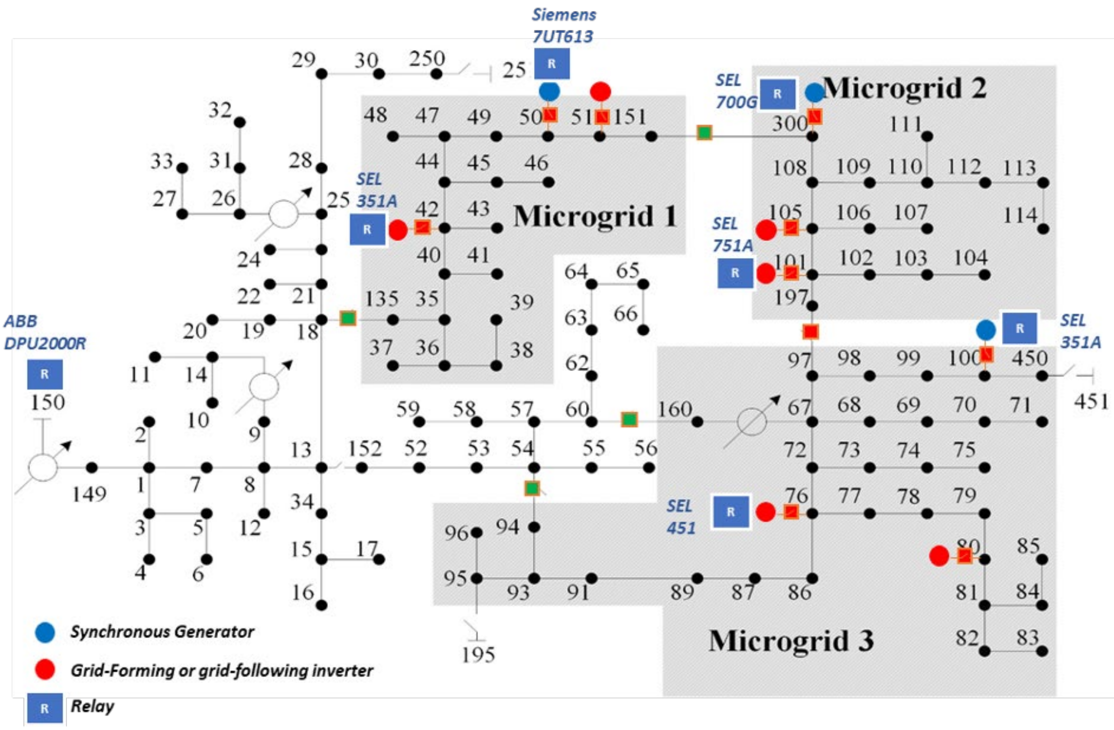

Figure 3: Single line representation of the modified IEEE 123-bus networked microgrid.

The validation study consists of three steps.

1. The first step involves learning the nominal behavior of the underlying power network. This is achieved by making some selective reference real power set point changes at the inverters. Then, applying Koopman operator theory, we learn the system dynamics.
2. Applying the resilience ratio metric on the nominal system, we mimic losing an inverter and identify which one results in a relatively less resilient state.
3. Actual fault scenarios are created at the inverters and the corresponding data is obtained. The recovery energy metric is then applied on the fault data and the corresponding energies are calculated.

Finally, the estimated resilience of losing each inverter is compared against the recovery energy required to reach the desired operating state to understand the applicability of the proposed resilience metrics and validate the estimated resilience findings.

3.1 System Identification

In total, we made 4 different reference set-point changes from the nominal set-point by increasing and decreasing it at each inverter. Therefore, we obtained 24 datasets to learn the Koopman-based dynamical system for the 123-bus system. We refer this data as the *training data*.

The real power and frequency measurements are considered as states and the reference power input is considered to be the input to learn the controlled dynamical system using Koopman operator theory. The time-series data corresponding to a set-point change at each inverter are shown in Figs. 4 - 9 and the eigenvalues of the learned Koopman operator are shown in Fig. 10.

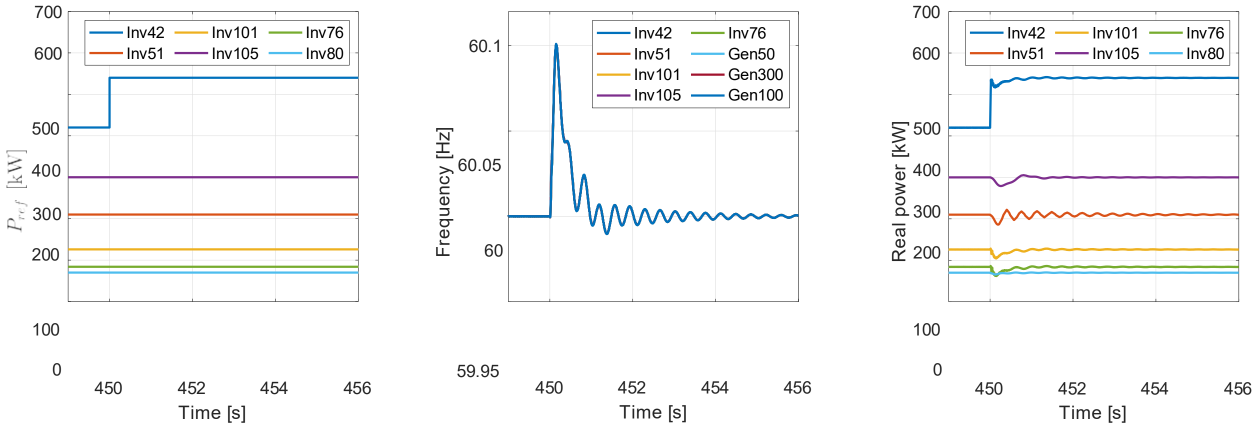

Figure 4: Time-series data corresponding to the Inverter 1 set-point change.

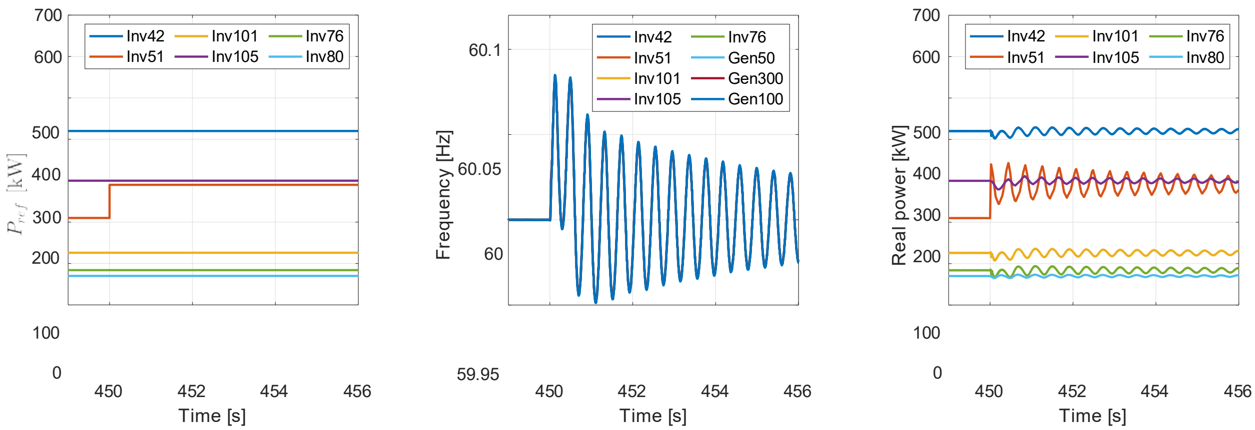

Figure 5: Time-series data corresponding to the Inverter 2 set-point change.

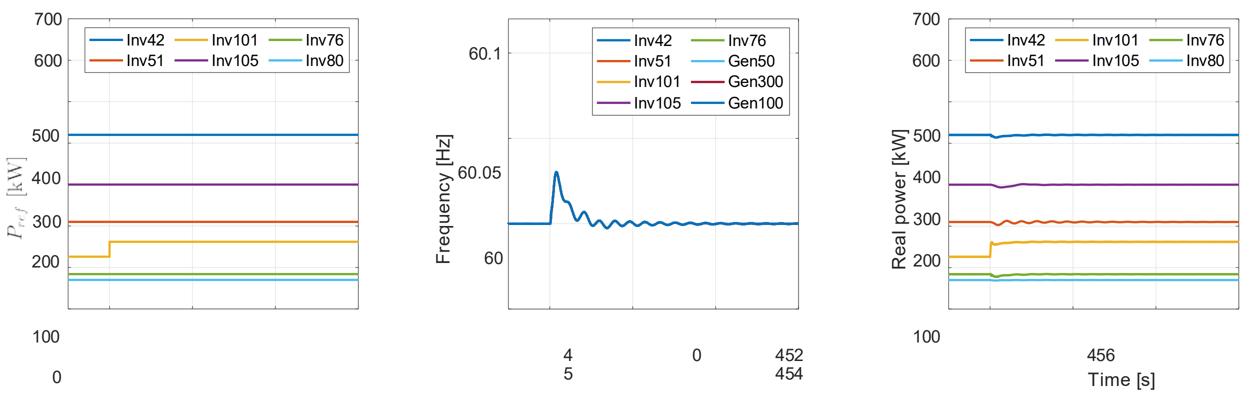

59.95

450
52
54
56

4
4
4
T
i
m
e
[
s
]

0

450

452
454
456
Time
[s]

Figure 6: Time-series data corresponding to the Inverter 3 set-point change.

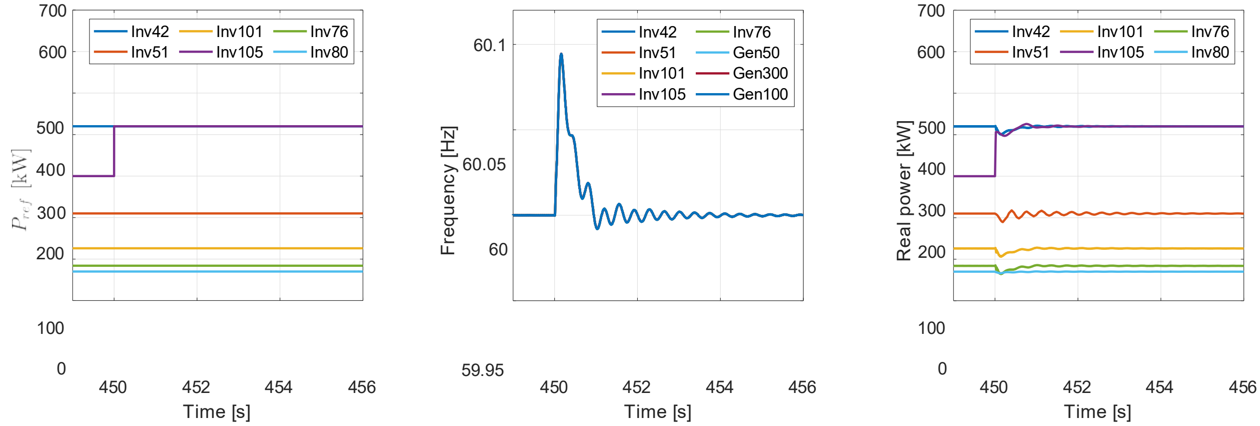

Figure 7: Time-series data corresponding to the Inverter 4 set-point change.

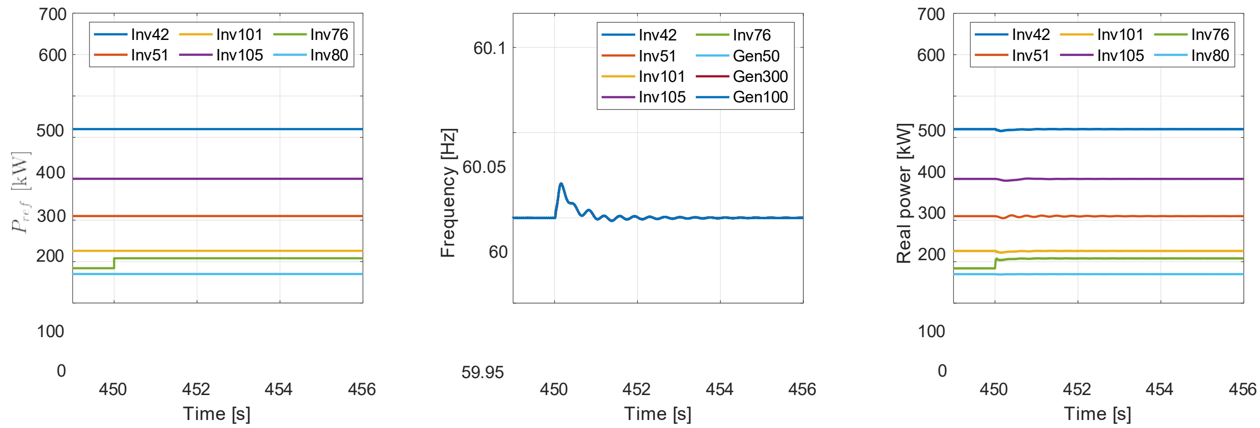

Figure 8: Time-series data corresponding to the Inverter 5 set-point change.

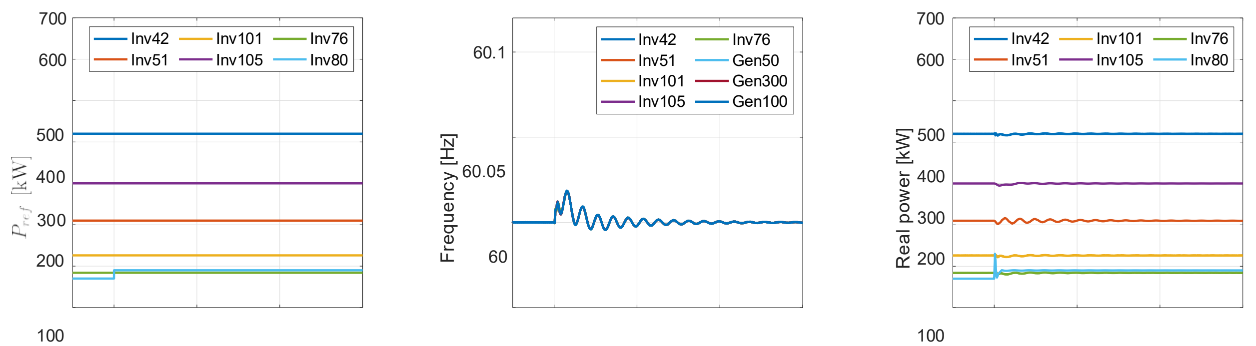

Figure 9: Time-series data corresponding to the Inverter 6 set-point change.

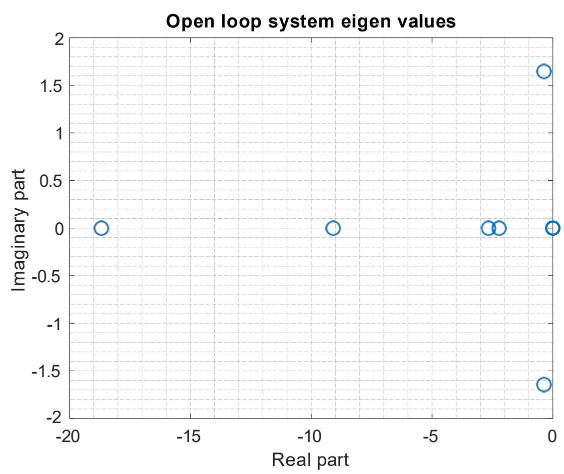

Figure 10: Eigenvalues of the Koopman Operator

3.2 Estimated Resilience Applying the Resilience Ratio

Once the system is identified, one can perform resilience analysis proactively by mimicking losing an actuator or a sensor and study/analyze the resilience with respect to that by calculating the resilience ratio. The corresponding resilience ratio values comparing with the size of the inverter are shown in the bar plot in Fig. 11.

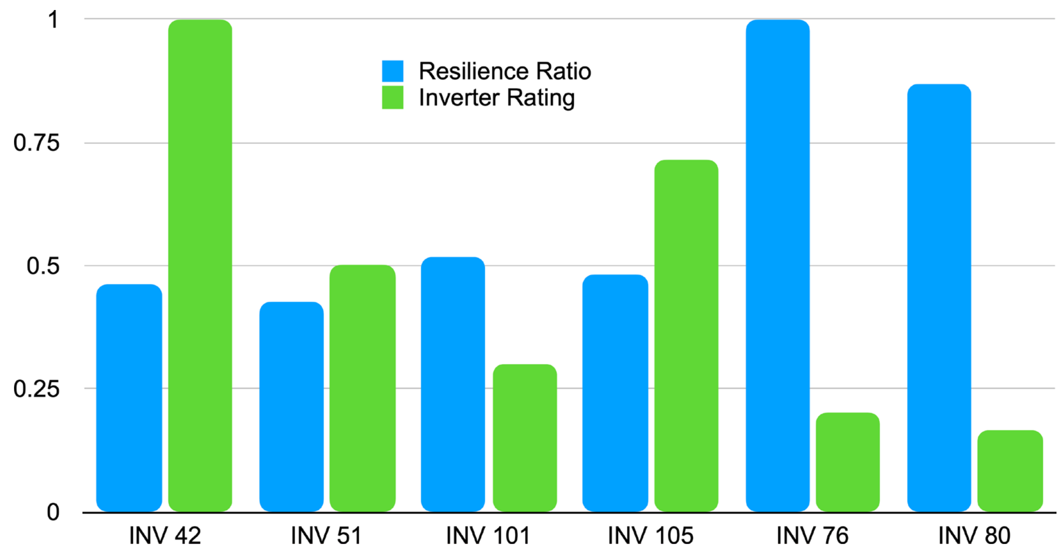

Figure 11: Resilience ratio of losing each inverter.

The bar plots in Fig. 11 are normalized with respect to their maximum values for both resilience ratio as well as the inverter rated power. The immediate observations from Fig. 11 are as follows. Losing the smallest inverters such as INV 76 and INV 80 does not result in a significant change in the resilience ratio, however, losing the largest inverter (INV 42) significantly impacts the resilience. One important remark which is not strictly following our immediate observation, is that losing INV 51 commits the smallest resilience ratio while it only receives the third largest inverter rating, even though the resilience ratio of the largest inverter (INV42) and INV 51 are very close. Therefore, this analysis shows that it is not trivial to identify the inverter locations that are least (highly) resilient.

3.3 Actual Resilience Applying the Recovery Energy

Here, we actually create fault scenarios at the inverters and obtain the corresponding data. An initial condition from the fault recovery window is chosen to compute the minimal energy it takes to reach the desired operating state and maintain it there.

The fault data is generated on the HYPERSIM such that we lose one inverter at a time. The corresponding time-series data are shown in Figs. 12 - 17.

The recovery energy corresponding to all the 6 cases is shown in Fig. 18. The recovery energy values are compared against the resilience ratios and both are normalized with respect to their maximum values correspondingly.

It is clear from Fig. 18 that the inverters with highest resilience ratios require the smallest energy to recover (see at INV 76 and INV 80). Contrarily, the inverter with least resilience ratio has the largest recovery energy.

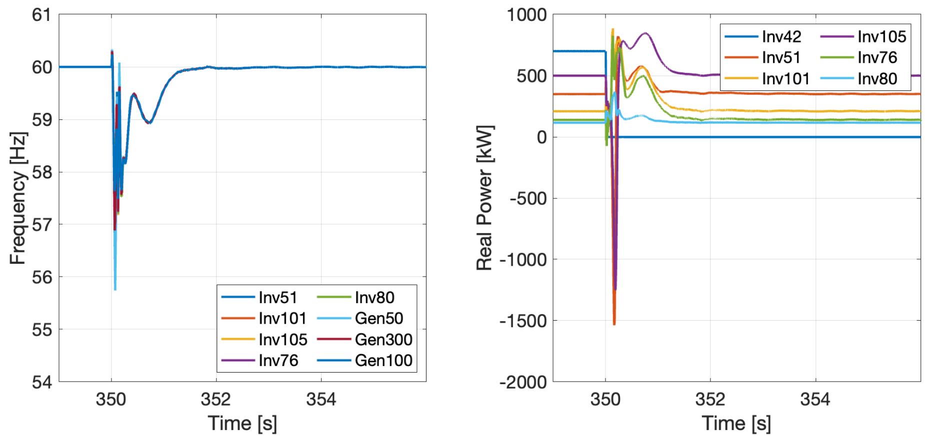

Figure 12: Data corresponding to fault at Inverter 1.

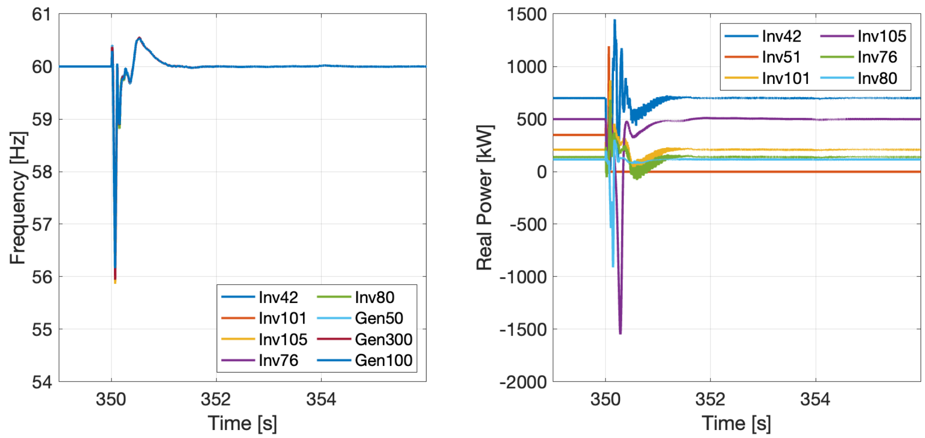

Figure 13: Data corresponding to fault at Inverter 2.

The above simulation experiments validates the complimentary aspects of the proposed resilience metrics and brings in their applicability to power systems.

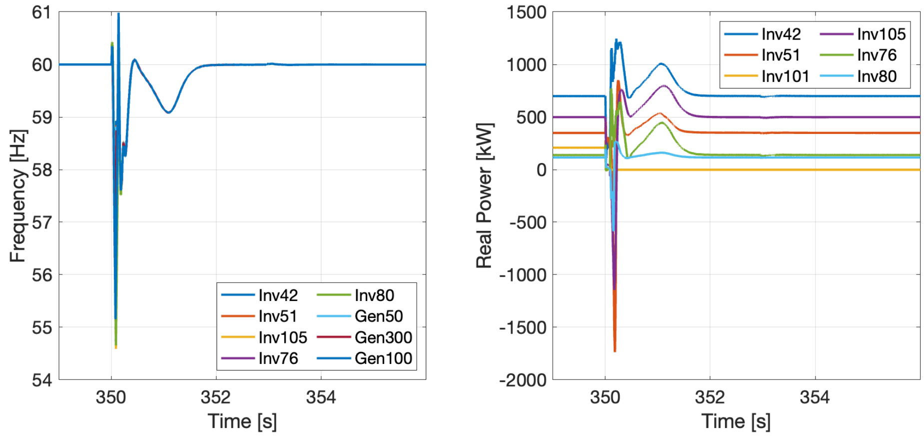

Figure 14: Data corresponding to fault at Inverter 3.

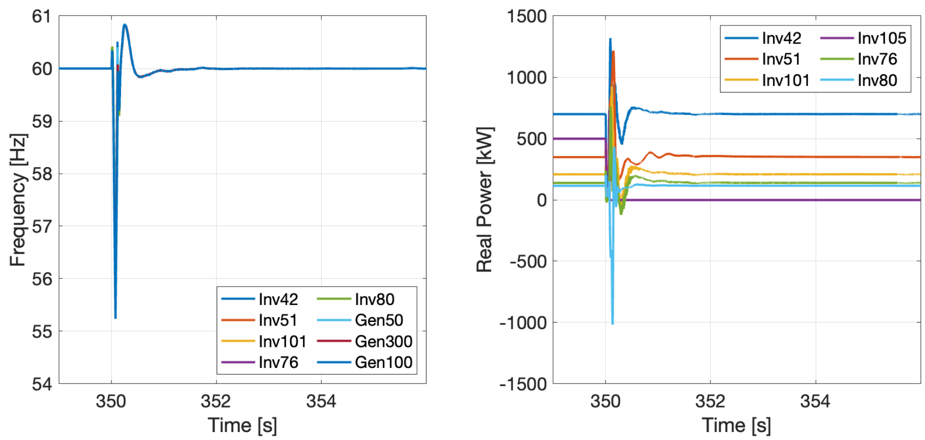

Figure 15: Data corresponding to fault at Inverter 4.

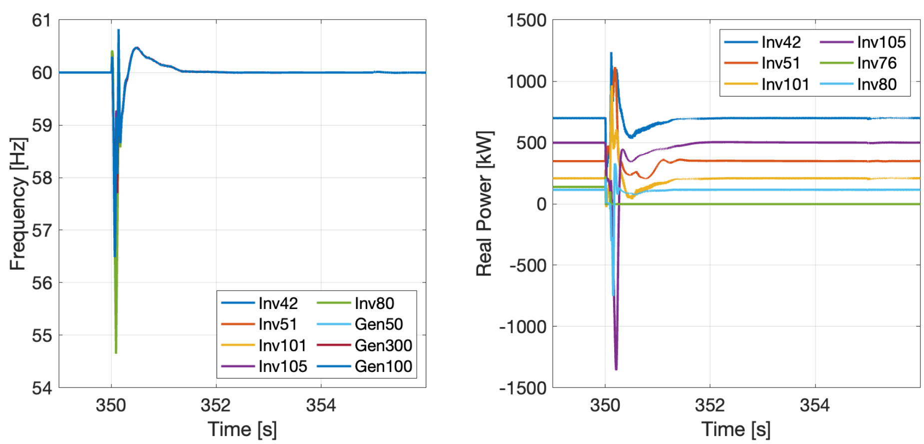

Figure 16: Data corresponding to fault at Inverter 5.

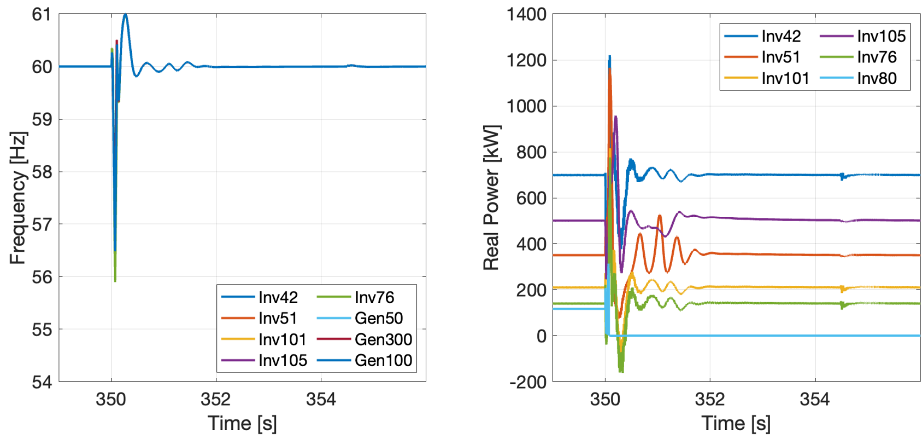

Figure 17: Data corresponding to fault at Inverter 6.

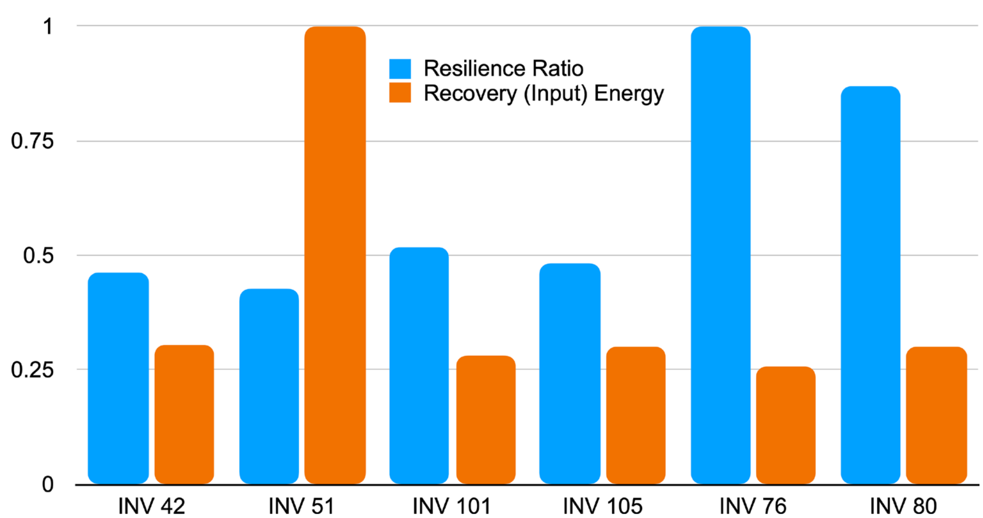

Figure 18: Recovery energy after losing each inverter.

4.0 Conclusion

In this project, we provided two definitions of resiliency of a control dynamical system. The first definition captures how easy (hard) it is to control and observe the system. For linear systems this can be quantified in terms of the controllability and observability Gramians and to extend this for nonlinear systems, we used the Koopman operator framework. This is because the evolution of the Koopman system is always linear, albeit in the space of functions. This linear representation allows us to define controllability and observability Gramians for a class of nonlinear systems and thus one can quantify resiliency for a nonlinear system. The second formulation uses the concept of recovery energy of a dynamical system and we showed, via numerical simulations, that both these metrics are consistent with each other and give the same conclusions.

5.0 References

[1] G. Kandaperumal, A. K. Srivastava, Resilience of the electric distribution systems: concepts, classification, assessment, challenges, and research needs, IET Smart Grid 3 (2) (2020) 133–143.

[2] S. Sinha, S. P. Nandanoori, T. Ramachandran, C. Bakker, Data-driven resilience characterization of control dynamical systems, in: 2022 American Control Conference, 2022 [Accepted].

[3] R. Arghandeh, A. Von Meier, L. Mehrmanesh, L. Mili, On the definition of cyber-physical resilience in power systems, Renewable and Sustainable Energy Reviews 58 (2016) 1060–1069.

[4] A. Clark, S. Zonouz, Cyber-physical resilience: Definition and assessment metric, IEEE Transactions on Smart Grid 10 (2) (2017) 1671–1684.

[5] C. G. Rieger, Resilient control systems practical metrics basis for defining mission impact, in: 2014 7th International Symposium on Resilient Control Systems (ISRCS), IEEE, 2014, pp. 1–10.

[6] Y. Wang, Resilience quantification for probabilistic design of cyber-physical system networks, ASCE-ASME J Risk and Uncert in Engrg Sys Part B Mech Engrg 4 (3) (2018).

[7] C. Rougé, J.-D. Mathias, G. Deffuant, Extending the viability theory framework of resilience to uncertain dynamics, and application to lake eutrophication, Ecological indicators 29 (2013) 420–433.

[8] Q. Zhu, T. Başar, Robust and resilient control design for cyber-physical systems with an application to power systems, in: 2011 50th IEEE Conference on Decision and Control and European Control Conference, IEEE, 2011, pp. 4066–4071.

[9] M. d. Lara, et al., A mathematical framework for resilience: dynamics, uncertainties, strategies, and recovery regimes., Environmental Modeling & Assessment 23 (6) (2018) 703–712.

[10] C. Bakker, A. Bhattacharya, S. Chatterjee, C. J. Perkins, M. R. Oster, The Koopman Operator: Capabilities and Recent Advances, in: 2020 Resilience Week (RWS), IEEE, 2020, pp. 34–40.

[11] A. Lasota, M. C. Mackey, Chaos, Fractals, and Noise: Stochastic Aspects of Dynamics, Applied Mathematical Sciences, Springer-Verlag New York, 1994.

[12] S. Sinha, S. P. Nandanoori, E. Yeung, Koopman operator methods for global phase space exploration of equivariant dynamical systems, IFAC-PapersOnLine 53 (2) (2020) 1150–1155.

[13] S. Sinha, B. Huang, U. Vaidya, On robust computation of Koopman operator and prediction in random dynamical systems, Journal of Nonlinear Science 30 (5) (2020) 2057–2090.

[14] S. P. Nandanoori, S. Sinha, E. Yeung, Data-driven operator theoretic methods for phase space learning and analysis, Journal of Nonlinear Science 32 (6) (2022) 95.

[15] A. Mauroy, I. Mezić, Global stability analysis using the eigenfunctions of the Koopman operator, IEEE Transactions on Automatic Control 61 (11) (2016) 3356–3369.

[16] A. Surana, Koopman operator based observer synthesis for control-affine nonlinear systems, in: 2016 IEEE 55th Conference on Decision and Control (CDC), IEEE, 2016, pp. 6492–6499.

[17] C. Bakker, W. S. Rosenthal, K. E. Nowak, Koopman representations of dynamic systems with control, arXiv preprint arXiv:1908.02233 (2019).

[18] C. Folkestad, D. Pastor, I. Mezić, R. Mohr, M. Fonoberova, J. Burdick, Extended dynamic mode decomposition with learned Koopman eigenfunctions for prediction and control, in: 2020 american control conference (ACC), IEEE, 2020, pp. 3906–3913.

[19] J. L. Proctor, S. L. Brunton, J. N. Kutz, Dynamic mode decomposition with control, SIAM Journal on Applied Dynamical Systems 15 (1) (2016) 142–161.

[20] X. Ma, B. Huang, U. Vaidya, Optimal quadratic regulation of nonlinear system using koopman operator, in: 2019 American Control Conference (ACC), IEEE, 2019, pp. 4911–4916.

[21] E. Yeung, Z. Liu, N. O. Hodas, A Koopman operator approach for computing and bal- ancing gramians for discrete time nonlinear systems, in: 2018 Annual American Control Conference (ACC), IEEE, 2018, pp. 337–344.

[22] A. Surana, Koopman operator framework for time series modeling and analysis, Journal of Nonlinear Science 30 (5) (2020) 1973–2006.

[23] A. Mauroy, I. Mezić, J. Moehlis, Isostables, isochrons, and Koopman spectrum for the action–angle representation of stable fixed point dynamics, Physica D: Nonlinear Phenomena 261 (2013) 19–30.

[24] Y. Susuki, I. Mezić, Nonlinear Koopman modes and power system stability assessment without models, IEEE Transactions on Power Systems 29 (2) (2013) 899–907.

[25] S. P. Nandanoori, S. Kundu, S. Pal, K. Agarwal, S. Choudhury, Model-agnostic algorithm for real-time attack identification in power grid using koopman modes, in: 2020 IEEE International Conference on Communications, Control, and Computing Technologies for Smart Grids (SmartGridComm), IEEE, 2020, pp. 1–6.

[26] S. Sinha, S. P. Nandanoori, T. Ramachandran, C. Bakker, A. Singhal, Data-driven resilience characterization of control dynamical systems, in: 2022 American Control Conference (ACC), IEEE, 2022, pp. 2186–2193.

[27] T. Ramachandran, S. P. Nandanoori, S. Sinha, C. Bakker, Data-driven characterization of recovery energy in controlled dynamical systems using koopman operator, in: 2022 IEEE 61st Conference on Decision and Control (CDC), IEEE, 2022, pp. 2230–2235.

[28] R. Jinsiwale, M. Maharjan, T. Becejac, A. Ashok, Evaluating a real-time model decoupling compensation approach for developing scalable, high-fidelity microgrid models, in: 2023 IEEE Texas Power and Energy Conference (TPEC), IEEE, 2023, pp. 1–6.

Pacific Northwest National Laboratory

902 Battelle Boulevard
P.O. Box 999
Richland, WA 99352
1-888-375-PNNL (7675)

www.pnnl.gov